



Correlation of Elastohydrodynamic Friction with Molecular Structure of Highly Refined Hydrocarbon Base Oils

Hak Mook Kim^{1,2} · Hugh Spikes²

Received: 10 September 2019 / Accepted: 2 January 2020
© The Author(s) 2020

Abstract

The molecular compositions of a range of low viscosity hydrocarbon base oils spanning API Groups II to IV have been quantified using ¹³C NMR and correlated with base oil elastohydrodynamic (EHD) friction. A strong correlation has been found between the proportions of paraffin, linear and branched carbons and EHD friction, with a high proportion of linear and paraffinic carbon atoms contributing to low-EHD friction but branched carbons contributing to high-EHD friction. Correlation equations have been developed to predict EHD friction based on base oil composition. At very high temperature and low pressure, this correlation breaks down as the lubricant in the contact does not reach sufficiently high shear stress for shear thinning to occur. For Group IV polyalphaolefin, the correlation must be extended to account for the very high proportion of linear carbons originating from linear alkene oligomerization. The correlations developed in this study can be used to guide the design of low-EHD friction base oils.

Keywords EHD friction · Traction · Low friction · ¹³C NMR · API groups · Base oil structure

1 Introduction

To meet challenging carbon dioxide emissions reduction targets, coupled with increasing demands of electric vehicles whose transmissions are subjected to very high torque and thus high contact pressures, industry is increasingly demanding high quality base stocks with superior elastohydrodynamic (EHD) frictional characteristics. Base stock qualities depend primarily on the crude oil feedstock and the refining process technology employed, and these result in widely differing base oil structures, and thus properties and performance, including EHD friction.

Crude oils consist of mixtures of hydrocarbon molecules with primarily paraffinic, naphthenic and aromatic structures. They need to be refined to produce targeted base stocks suitable for lubricant applications. Since crude oils have both undesirable and desirable components, the

refining process needs to be a balance between removing, converting and retaining components to achieve an appropriate molecular structural transformation to the target product.

Vacuum gas oil or deasphalted oil from distillation of crude oil is generally used as feedstock to produce base stocks. Unlike Group I base stocks which are rich in aromatics and typically obtained from solvent processes, paraffinic base stocks are produced by catalytic hydroprocessing routes including hydrotreating, hydrocracking, isodewaxing and hydrofinishing. To obtain highly refined and highly paraffinic base stocks featuring high viscosity index, low cold cranking simulator (CCS) viscosity, better oxidation stability and higher boiling temperature, a combination of waxy feedstocks and severe hydroprocessing technology is typically adopted [1].

Elastohydrodynamic lubrication (EHL) is present in lubricated components such as gears, rolling bearing, cam-tappet systems and constant velocity joints, where non-conforming contacts generate high strain rate and very high pressure. EHD friction is determined by how the lubricant molecules respond to these conditions. It is now recognized that EHD friction is mainly affected by the structure and flexibility of the base oil molecules present, since these control how easily molecular layers move past one another

✉ Hak Mook Kim
mook@sk.com

¹ Institute of Technology Innovation, SK Innovation Co., Ltd, 325 Expo-ro, Yuseong-gu, Daejeon 34124, Republic of Korea

² Imperial College London, Tribology Group, London SW7 2AZ, UK

during shear at high pressure when the available free volume is very limited [2].

Although there have been many studies concerning the EHD friction properties of different base oils, these have mainly focused on synthetic base oils designed to provide high-EHD friction for traction drives [3, 4]. Studies of the EHD friction of conventional, petroleum-derived hydrocarbon base oils has been limited to exploring the impact of base oil viscosity and API group type, with little attempt to relate EHD friction to detailed base oil composition.

In this study, the EHD friction of low viscosity, highly refined paraffinic base oils such as are becoming prevalent in low-friction lubricant formulations is correlated with molecular structural parameters determined by ^{13}C nuclear magnetic resonance (NMR) spectroscopy. The aim is to better understand how to obtain low viscosity, hydrocarbon lubricants that provide low friction in EHD contacts.

2 Previous Work

There has been considerable previous research on the EHD friction properties of base fluids aimed at relating their friction behaviour to their composition. Gonsel and co-workers studied a wide range of base fluids from various refining processes and with different kinematic viscosities, and found that synthetic polyalphaolefin (PAO) and hydro-treated base oils gave lower friction than solvent-treated mineral base oils [5]. This has been recently confirmed by Zhang et al. [2].

Most systematic exploration of the relationship between EHD friction and molecular structure of base fluids has focused on synthetic base oils and especially fluids that deliver high-EHD friction [3, 4 6–11]. This is unsurprising since the molecular structure of most synthetics is much better defined than that of mineral oil-derived fluids. It has been shown that cyclic saturated ring structures give high-EHD friction [3, 6] and that the extent of alkyl chain branching also contributes to an increase of EHD friction [4]. Tsubouchi identified five key molecular structure features for high-EHD friction to be high molecular stiffness, large size, short alkyl chain length, high melting point and low molecular polarity [7–10]. Edgar and Hurley applied quantitative structure activity relationships (QSAR) to predict EHD friction based on friction measurements on a learning set of molecules of known structure to aid in the development of new traction fluids [11].

Oxygen-containing Group V synthetic base oils, such as esters and glycols have been another area of interest in terms of EHD friction behaviour. Hetchshel studied various polyglycols and found that ethylene-based ones gave the lowest EHD friction. He proposed that lubricant molecules with

a thread-like shape and a minimum of pendant structural subunits or functional groups reduced the intermolecular interactions that contribute to EHD friction [12]. Chang et al. found that shear stress (and thus friction) was strongly dependent on ester structure, demonstrating that esters with long and linear chains gave low shear stress, while branched chain esters gave relatively high shear stress [13]. Zhang et al. measured the EHD friction properties of a very wide range of base fluids including synthetics and mineral oils. They confirmed the importance of molecular structure of the base fluid on EHD friction and that liquids having linear-shaped molecules with flexible bonds give lower friction than liquids with bulky side groups or rings [2].

Most of the studies above have employed disc machines or ball-on-disc tribometers and were aimed specifically at measuring EHD friction. A number of studies have also explored the impact of lubricant molecular structure on the friction and efficiency of actual engineering components. Rounds used a thrust ball bearing rig to measure the friction properties of several mineral and synthetic base oils and found that naphthenic base oils gave higher friction than paraffinic base oils [14]. Yang et al. measured the temperature rise of a loaded thrust bearing to correlate with measured EHD friction. Based on this, they suggested that EHD friction is one of the important lubricant properties in determining rolling bearing efficiency and found that Group III+, IV and ester (Group V) have generally low-EHD friction [15]. Yoshizaki et al. studied the influence of base oil structures on friction loss by testing spur gears [16] while Höhn et al. investigated the influence of base oil type on gear mesh losses [17]. They both noted torque reduction with synthetic base oils including esters, polyglycols and PAO, compared to mineral base oils.

In this study, highly refined hydrocarbon base oils with quite similar compositional types have been selected to conduct a systematic study of the impact of molecular structure on EHD friction. Nuclear magnetic resonance (NMR) spectroscopy has been reported to be a powerful tool to understand the structural parameters of base oils and has been correlated with the latter's bulk properties such as low-temperature rheology and pressure-viscosity coefficient [18–22]. In this study, NMR has been applied to derive a range of quantitative structural parameters of the base oils of interest and a series of EHD friction property measurements has been made on the same set of base oils at various conditions. Finally, correlation by multiple regression fit has been made between the quantitative molecular structural characteristics and EHD friction. This correlation between structure and property can be used to inform the design of tailored molecules to create new base oils able to cope with the rising demand for high quality, low-friction base oils.

3 Test Fluids

The eleven hydrocarbon base oils used in this study are listed in Table 1. They include a range of Group II, III and IV base oils as classified by American Petroleum Institute (API) [23], with kinematic viscosities of around 4 centistokes (cSt) at 100 °C measured using the ASTM D445 test method. Although Group II+ and Group III+ are marketing terms generally expressed to differentiate higher VI base stocks within their own groups (Group II+ : VI 110–119, Group III+ : VI 130 or more), the base oil samples studied here were further classified based on their Viscosity Index (VI). PAO designated as Group IV was used as a synthetic hydrocarbon base oil.

4 Test Methods

4.1 EHD Friction

EHD friction was measured using a mini traction machine (MTM2, PCS Instruments). In the MTM, a ball is loaded against the flat surface of a disc immersed in lubricant and these are independently driven to enable any desired combination of rolling and sliding speed. Friction curves were obtained at a fixed entrainment speed of 2.0 m/s over a wide range of slide-roll ratio (SRR) values ramped up from 0 to 50%. In this study, 19.5 mm diameter AISI 52100 steel balls and 46 mm diameter AISI 52100 steel discs were employed. Their root mean square surface roughnesses, R_q , were 11 and 5.5 nm, respectively.

The tests were conducted at five different temperatures, 40, 60, 80, 100 and 120 °C, and four different applied loads, 15.0, 25.9, 41.1 and 61.3 N, corresponding to mean Hertz pressures of 0.5, 0.6, 0.7 and 0.8 GPa, respectively.

Table 1 Hydrocarbon base oils tested

| Base oil | KV40(cSt) | KV100(cSt) | VI |
|-----------|-----------|------------|-----|
| GrII | 19.87 | 4.068 | 103 |
| GrII+(A) | 22.87 | 4.588 | 116 |
| GrII+(B) | 21.20 | 4.406 | 119 |
| GrIII(A) | 19.50 | 4.235 | 124 |
| GrIII(B) | 20.04 | 4.285 | 121 |
| GrIII(C) | 19.57 | 4.273 | 126 |
| GrIII(D) | 21.17 | 4.474 | 125 |
| GrIII+(A) | 18.50 | 4.186 | 133 |
| GrIII+(B) | 18.03 | 4.090 | 130 |
| GrIII+(C) | 19.25 | 4.273 | 131 |
| GrIV | 17.93 | 4.031 | 125 |

4.2 EHD Film Thickness

The EHD film-forming properties of the test oils were also measured in order both to ensure that friction measurements were made in full-film EHD conditions and also to enable calculation of the mean shear rates present in the frictional contacts. EHD film thickness measurements were made using an ultrathin film measurement system (EHD2, PCS Instruments). This employs optical interferometry to measure lubricant film thickness in a rolling steel ball on coated disc contact [24].

In this study, the measurements of central film thickness were made as a function of entrainment speed in nominally pure rolling with a steel ball/glass disc combination at an applied load of 20 N.

4.3 Nuclear Magnetic Resonance Spectroscopy

^{13}C NMR analysis was carried out on a 600 MHz NMR spectrometer in deuterated chloroform. The experiments were performed at room temperature and chemical shifts were measured with respect to tetramethylsilane (TMS) used as an internal standard. Neat base oils were analyzed without separation of saturate and aromatic fractions. Structural parameters of the base oils were computed from the data obtained from ^{13}C NMR measurements.

5 Results

5.1 EHD Friction

Some of the EHD friction coefficient *versus* SRR curves obtained at different temperatures and pressures are presented in Fig. 1. All fluids were tested twice and all showed less than 5% variation between repeat tests under all conditions. All of hydrocarbon base oils showed a very similar pattern of frictional behaviour, where friction increased with pressure and decreased with temperature. There is an evident systematic variation of friction coefficient with API group except at very low pressure and high temperature.

5.2 EHD Film Thickness

Film thickness measurements were made on all the base oils over the temperature range 40 to 120 °C. Figure 2 shows results at 40 and 100 °C. These measurements were used to estimate the film thicknesses in the MTM friction tests. In this estimation, allowance was made for the effects of differences in elastic modulus and applied load between film thickness and friction measurements by using the Dowson and Hamrock film thickness equation [25]. They showed that

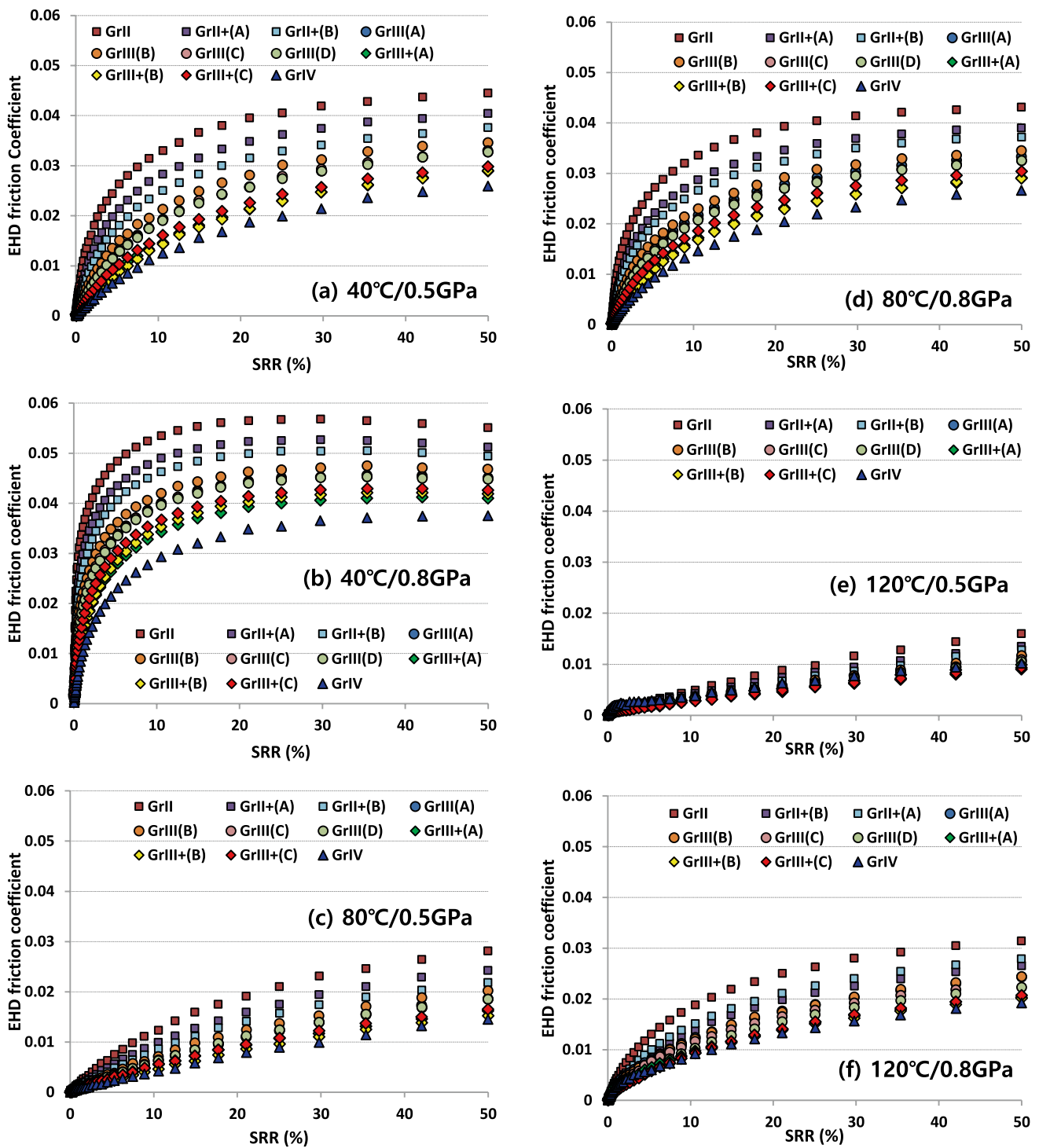


Fig. 1 EHD friction versus SRR for hydrocarbon base oils, a 40 °C/0.5GPa, b 40 °C/0.8GPa, c 80 °C/0.5GPa, d 80 °C/0.8GPa, e 120 °C/0.5GPa, f 120 °C/0.8GPa (The all set of EHD friction data shown in Appendix)

all subsequent MTM friction measurements were made in full-film EHD conditions with lambda ratio (ratio of central EHD film thickness to composite surface roughness) always greater than 4.

These film thickness data were also used to determine strain rates (sliding speed/film thickness) to enable conversion of EHD friction curves to plots of mean shear stress versus strain rate as described later in this paper.

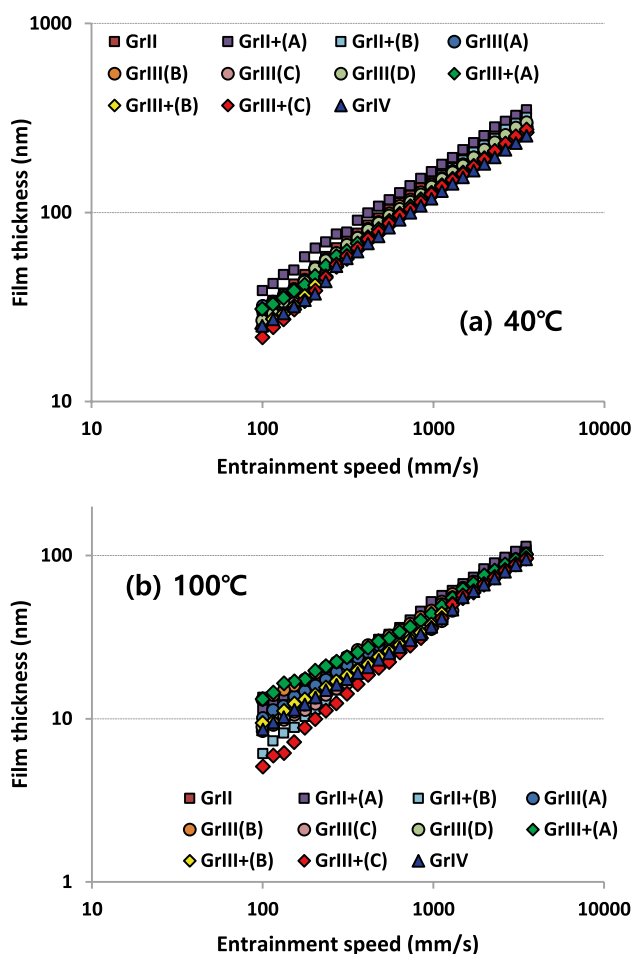


Fig. 2 EHD film thickness *versus* entrainment speed for hydrocarbon base oils, a 40 °C, b 100 °C

5.3 Nuclear Magnetic Resonance Spectroscopy

A ^{13}C NMR spectrum of one of the base oils is shown in Fig. 3. The quantitative ^{13}C NMR provides important details on the different types of carbon atoms present in the average structure of base oils. Therefore, it gives a compositional profile for each base oil including detailed paraffinic structure estimation. The general assignment of all of the peaks in ^{13}C NMR spectra was carried out based on earlier studies [18–22].

The carbons are first divided into saturated (C_{SAT} , 5–60 ppm) and aromatic (C_{ARO} , 90–160 ppm) types. As most of the base oils studied here are highly refined base oils, saturated carbon atoms are divided into paraffin carbons and naphthenic carbons to identify specific saturate carbon structures. Naphthenic carbons are poorly resolved in ^{13}C NMR spectroscopy, which results in a broad hump in the 24–60 ppm region. Therefore, a baseline correction

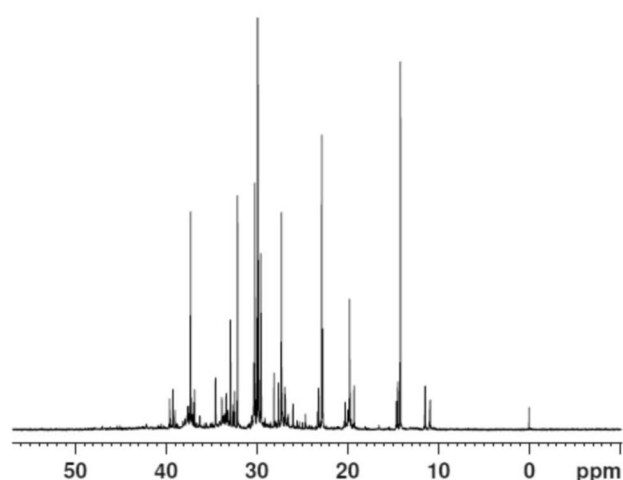


Fig. 3 ^{13}C NMR spectrum of hydrocarbon base oil GrIII(A)

was applied to remove the naphthenic carbon background. Paraffin carbons are then further divided into linear carbons and branched carbons. Linear carbon content is determined by integrating terminal carbons on long alkyl chains with carbon atoms located 1, 2, 3 and 4 or more carbon atoms away from a terminal carbon. These are indicated as α , β , γ , δ , and ϵ in Fig. 4(a) and ^{13}C NMR peaks of these are at 14.1, 22.9, 32.1, 29.6 and 29.9 ppm, respectively. Not included as linear carbons are those within three carbons of a tertiary carbon, as indicated by α' , β' , γ' in Fig. 4a. Branched carbons are determined by integrating carbons in branched environments consisting of the total of pendant and terminal carbons in methyl, ethyl, propyl and butyl groups as illustrated in Fig. 4b. These correspond to 19.2–20.1 ppm (3 and more-Me), 22.6–22.8 ppm (2-Me), 10.9–11.6 ppm (Et), 14.4–14.8 ppm (Pr), and 23.2–23.4 ppm (Bu).

The measured values of the above three derived structural parameters are listed in Table 2 for all the base oils except for the PAO which will be discussed separately in the discussion section.

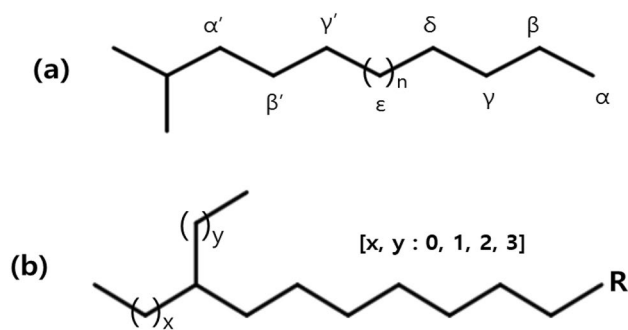


Fig. 4 Paraffinic structures of hydrocarbon base oil

Table 2 ^{13}C NMR structural parameters of hydrocarbon base oils

| | GrII | GrII+(A) | GrII+(B) | GrIII(A) | GrIII(B) | GrIII(C) | GrIII(D) | GrIII+(A) | GrIII+(B) | GrIII+(C) |
|-------------------------------|------|----------|----------|----------|----------|----------|----------|-----------|-----------|-----------|
| Paraffin carbons (C_p), % | 53.6 | 64.7 | 68.4 | 73.7 | 72.5 | 76.0 | 80.0 | 84.8 | 92.3 | 82.0 |
| Branched carbons (C_B), % | 8.1 | 6.7 | 6.7 | 8.8 | 8.8 | 9.2 | 10.1 | 10.6 | 12.0 | 8.1 |
| Linear carbons (C_L), % | 20.9 | 23.9 | 24.7 | 29.3 | 28.2 | 30.2 | 29.2 | 31.8 | 31.0 | 29.8 |

6 Discussion

6.1 Shape of EHD Friction Curves

At most temperatures and loads, the friction coefficient *versus* SRR curves as illustrated in Fig. 1 show classical EHD friction behaviour, with a rapid rise in friction with SRR followed at higher SRR by a levelling out and then, at the highest loads, a slight drop in friction coefficient. Johnson and Tewaarwerk have produced the most widely accepted model of this behaviour [26]. At very low SRR and thus low strain rates, the fluid behaves in a Newtonian fashion, though this tends to be overlain at high pressures with an accommodation of some of the strain by a viscoelastic response of the fluid and elastic shear compliance of the contacting surfaces. When the strain rate and thus the shear stress reaches a critical value, often called the Eyring stress, the film starts to shear thin so that its shear stress no longer rises linearly with strain rate and this is responsible for the initial levelling out of the friction curves. At high shear stress and strain rate, the fluid film experiences a significant temperature rise due to shear heating, and this produces a full levelling out and even slight fall in the friction at high SRRs for most lubricants, including the ones tested in this study.

If EHD film thickness is known, friction coefficient *versus* SRR curves can be converted to graphs of mean shear stress (mean pressure multiplied by friction coefficient) *versus* strain rate (sliding speed divided by film thickness). This is shown in Fig. 5 for the two sets of friction curves at 40 °C in Fig. 1. In this figure, the graphs are plotted *versus* log (strain rate) and this shows approximately linear behaviour at high strain rate. This is as predicted by the Eyring-activated shear model which states that [26];

$$\bar{\tau} = \tau_e \sin h^{-1} \left(\frac{\eta_p \dot{\gamma}}{\tau_e} \right) \quad (1)$$

where τ_e is the Eyring stress above which shear thinning occurs, η_p is the low shear rate viscosity of the lubricant at the prevailing pressure and $\dot{\gamma}$ is the strain rate [27].

At shear stresses greater than about $1.5\tau_e$ this simplifies to;

$$\bar{\tau} = \tau_e \log_e \left(\frac{2\eta_p \dot{\gamma}}{\tau_e} \right) \quad (2)$$

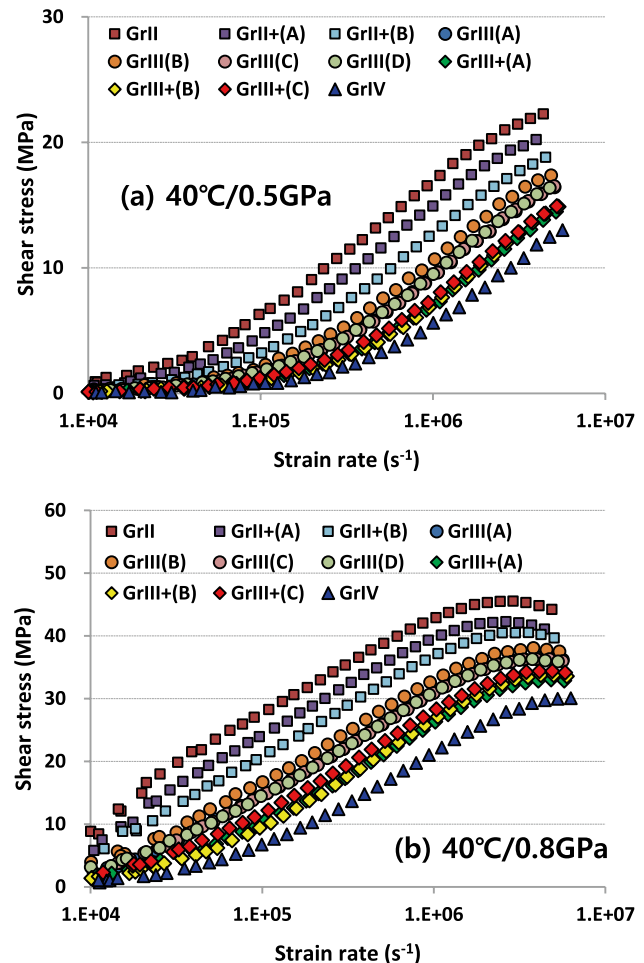


Fig. 5 EHD shear stress *versus* strain rate curves for hydrocarbon base oils, **a** 40 °C/0.5GPa, **b** 40 °C/0.8GPa

6.2 Isothermal Correction

Figure 5 shows that over much of the SRR range, mean shear stress is proportional to log (strain rate) but that at high strain rate the shear stress curves flatten and at high pressures, actually start to fall. This is due to shear heating of the EHD film at a combination of high shear stress and high strain rate. To determine the intrinsic EHD friction of base oils the effects of shear heating of the EHD film can be subtracted to obtain isothermal shear stress *versus* strain rate curves.

The mean temperature rise of oil film in a contact is the sum of the mean “flash temperature rise” of the two solid surfaces as they pass through the contact, $\Delta \bar{T}_{surf}$, and the mean temperature rise of the oil film above this surface temperature $\Delta \bar{T}_{oil}$, giving the mean oil film temperature in the contact, $\bar{T}_{oil\ film}$ as;

$$\bar{T}_{oil\ film} = T_o + \Delta \bar{T}_{surf} + \Delta \bar{T}_{oil} \tag{3}$$

$$= T_o + \frac{1}{(2\pi K_s \rho c^{0.5})} \left(\frac{2b}{U}\right)^{0.5} \dot{q}'' + \frac{h_c}{8K_{oil}} \dot{q}'' \tag{4}$$

where T_o is the bulk temperature, K_s , ρ and c are the thermal conductivity, density and specific heat of the surfaces, respectively, b is the contact half width and K_{oil} the thermal conductivity of the oil film. \dot{q}'' is the rate of heat generation by friction per unit area of film and is given by

$$\dot{q}'' = \frac{Fu_s}{A} = \bar{\tau} u_s = \bar{\tau} \dot{\gamma} h_c \tag{5}$$

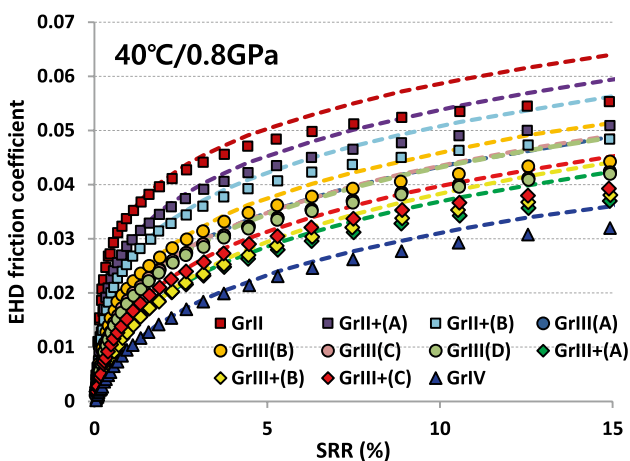
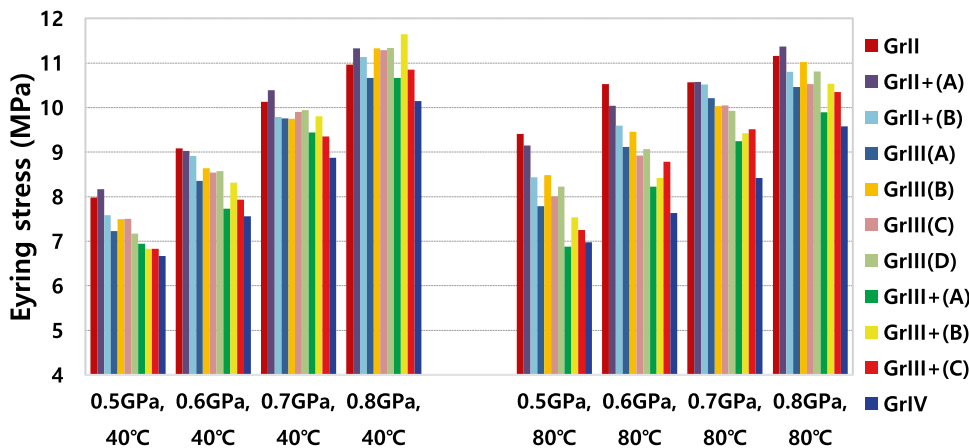


Fig. 6 Isothermally corrected EHD friction versus SRR for hydrocarbon base oils; dashed lines are isothermally corrected values

Fig. 7 Calculated Eyring stress for hydrocarbon base oils



In Eq. 4, $K_s \rho c = 7.95 \times 10^7 \text{ J}^2 \text{ K}^{-2} \text{ s}^{-1} \text{ m}^{-4}$, b was $98 \mu\text{m}$ at a load of 15 N , $118 \mu\text{m}$ at 25.9 N , $137 \mu\text{m}$ at 41.1 N and $157 \mu\text{m}$ at 61.3 N . K_{oil} was estimated from data in [28] by selecting the nearest fluid type and correcting to the relevant mean contact pressures. For each measured friction value, the mean oil film temperatures in the contact calculated and mean shear stresses obtained from measured friction data were corrected back to their bulk test temperatures as described in [2].

Figure 6 shows the effect of this correction to isothermal conditions for a set of friction data. It can be seen that the correction has the effect of extending the logarithmic response region to higher strain rate, confirming the fit of the data to the Eyring shear thinning model. It does not change the ranking order of the various base oils in terms of their EHD friction.

6.3 Eyring Stresses

Figure 7 shows calculated Eyring stress for hydrocarbon base oils tested in this study. Some of these were used to predict friction coefficient, and then compared with isothermally corrected friction curves of base oils, as shown in Figs. 9 and 10.

6.4 Friction Behaviour at High Temperature and Low Load

As can be seen in Fig. 1e, at very low pressure and high temperature, the friction coefficient versus SRR curves are almost linear and there is relatively little difference in friction between the different groups. This is because under these conditions, all the fluids are behaving in a predominantly Newtonian fashion and do not reach sufficiently high shear stress to experience shear thinning. In this case dynamic viscosity alone will control friction. Evans and Johnson have derived regime maps to describe lubricant film rheological response at different pressures and strain rates

[29, 30]. These suggest that fluids behave in a Newtonian fashion at low strain rates, if they have low viscosity or are at modest pressure, but that in high pressure contacts, they show a shear-thinning response.

Figure 8 shows two sets of isothermally corrected shear stress *versus* strain rate data. The main graphs show shear stress *versus* log (strain rate) while the insets show shear stress *versus* linear strain rate. At high pressure and low temperature, the plots show that mean shear stress is proportional to log (strain rate). At low pressure and high temperature, however, the shear stress *versus* log strain rate curves are certainly not linear. Instead shear stress is proportional to strain rate suggesting little if any shear thinning in the EHD contact.

Figures 9 and 10 compare isothermally corrected, measured friction curves with calculated ones. Figure 9 is for EHD friction measured at low temperature and high pressure (61 N and 40 °C). This is compared with two predictions, one assuming that the fluid experiences an exponential rise in viscosity with pressure but does not shear thin. The second allows both a piezoviscous response and also

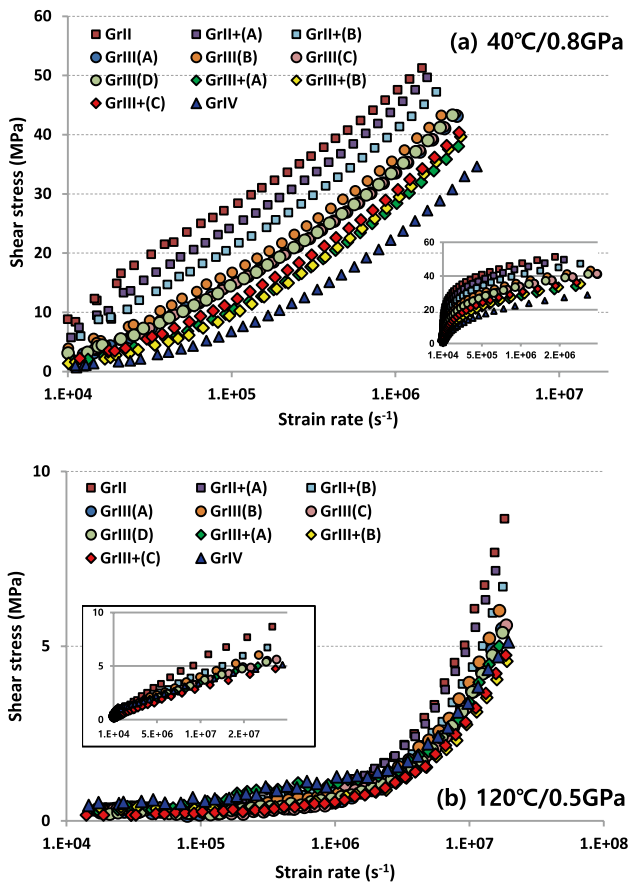


Fig. 8 Isothermally corrected EHD shear stress *versus* log₁₀ (strain rate) curves for hydrocarbon base oils, **a** 40 °C/0.8GPa, **b** 120 °C/0.5GPa. The insets show linear shear stress *versus* strain rate plots

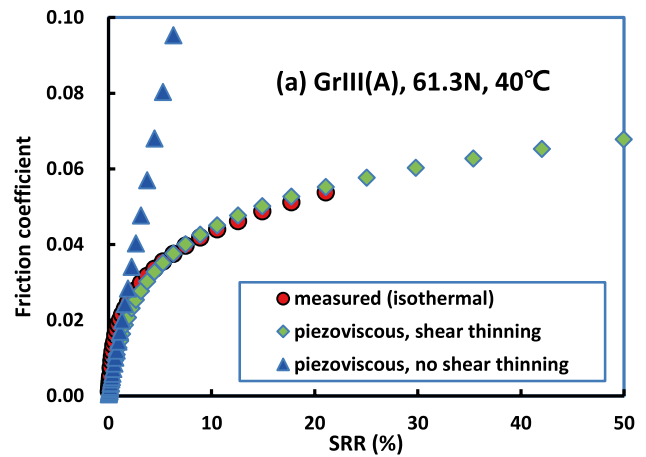


Fig. 9 Comparison of isothermally corrected friction curve of GrIII(A) base oil at high pressure and low temperature with predicted curves based on (i) piezoviscous, Newtonian and (ii) piezoviscous Eyring shear-thinning response

shear thinning according to the Eyring equation. For both predictions, the pressure-viscosity coefficient was taken to be 11 GPa⁻¹ and in the shear-thinning prediction an Eyring stress of 11.7 MPa was used, as determined from the slope of the measured curve at high shear rate. It is evident that measured friction results from a fluid that is experiencing both piezoviscous response and shear-thinning response. By contrast, Fig. 10 shows that at low pressure and high temperature using a pressure-viscosity coefficient of 10 GPa⁻¹, the friction can be predicted solely from a piezoviscous response without any shear thinning.

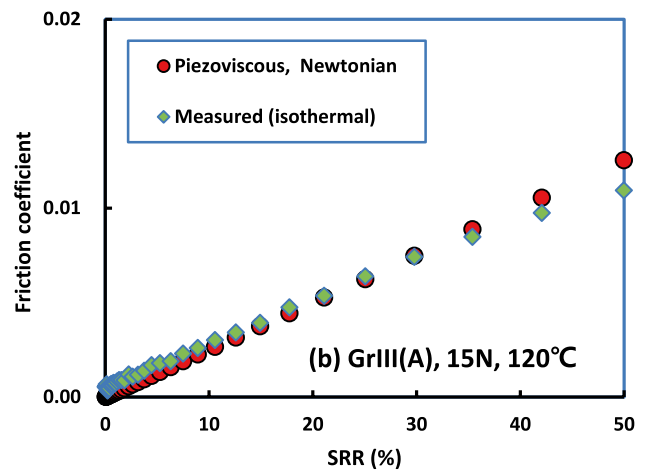


Fig. 10 Comparison of isothermally corrected friction curves of GrIII(A) base oil at low pressure and high temperature with predicted curve based on piezoviscous, Newtonian response

6.5 Correlation of EHD Friction and Structural Parameters

It is evident from Fig. 1 that base oil groups Group III, III+ and IV show relatively low-EHD friction. As suggested by previous researchers [2, 5, 6, 12, 13] this can be attributed to more linear paraffinic molecular structures in higher base oil groups, which enable easier alignment and less interaction with neighboring molecules during shear at high pressure, thus favouring lower EHD friction. In the current study, detailed structural parameters for each base oil were obtained using ^{13}C NMR as listed in Table 2 and multiple linear regression analysis of these parameters with EHD friction was carried out to model the relationship between them. Correlations were made for EHD frictions measured at each temperature and pressure at five different SRR values of 5, 10, 20, 30 and 50%. As expected, the parameters of total paraffin carbons and linear carbons are positively correlated with EHD friction, but the parameter of branch carbons is negatively correlated.

Detailed results of regression analysis are presented in Table 3. Very close correlations with R^2 coefficient of over 0.99 are obtained with EHD friction measured at 0.7 GPa and 0.8 GPa at 80 °C and 0.8 GPa at 100 °C, while the average R^2 for all EHD frictions measured was 0.968 and increased to 0.984 except for results measured at combined low pressure and high temperature (0.5 GPa and 0.6 GPa at 120 °C and 0.5 GPa at 100 °C). As indicated above in these last three conditions, although the contact is operating in the EHD regime, the shear stress in the contact is not high enough to cause shear thinning. Therefore all the fluids behave in a predominantly piezoviscous Newtonian fashion and do not reach sufficiently high shear stress to experience

shear thinning. To clarify the relative contribution of the three parameters, Table 4 shows the same fits but in normalized form. This shows that the linear carbons make the strongest contribution and also that branched carbons have a more significant effect at low than at high SRR.

Although the effects of molecular structure on EHD friction such as more linear chains and less branches to give lower EHD friction, have been reported mainly qualitatively, this study has clearly shown the effect of molecular structures quantitatively and a high degree of correlation based on detailed molecular carbon level. Thus, the findings could be applied to design lower EHD friction base oils to maximize fuel economy and energy efficiency.

The above correlations were made using the raw EHD friction data without thermal correction. Correlations were also tested using isothermally corrected friction data. The isothermally corrected average R^2 coefficient was 0.964 and increased to 0.984 when results measured at 0.5 GPa and 0.6 GPa at 120 °C, and 0.5 GPa at 100 °C were excluded. These are almost identical to the uncorrected friction correlations of 0.968 and 0.984. This is unsurprising since the isothermal correction is based on friction in a systematic way and should scale linearly with friction.

6.6 EHD Friction and Structural Parameters of PAO

PAO has been included in this study to compare the effectiveness of the correlation for synthetic hydrocarbon base oils that have considerably different structures from mineral base oils. As generally recognized, PAO shows relatively low-EHD friction based on a very high proportion of linear paraffin chains. Although PAO is synthesized paraffinic base oil, ^{13}C NMR structural parameters showed

Table 3 Detailed result of regression analysis relating EHD friction to ^{13}C NMR structural parameters of base oils (in these regression equations, C_p , C_L and C_B are fractional values, not percentages as in Table 2)

| $T(^{\circ}\text{C})$ | $P(\text{GPa})$ | SRR (%) | R^2 | Regression equation |
|-----------------------|-----------------|---------|-------|--|
| 40 | 0.6 | 5 | 0.986 | $0.0716 - 0.0258C_p - 0.117C_L + 0.0276C_B$ |
| | | 10 | 0.983 | $0.0774 - 0.0275C_p - 0.112C_L + 0.0289C_B$ |
| | | 30 | 0.979 | $0.0800 - 0.0230C_p - 0.101C_L + 0.0313C_B$ |
| | | 50 | 0.982 | $0.0767 - 0.0215C_p - 0.0848C_L + 0.0290C_B$ |
| 60 | 0.6 | 5 | 0.990 | $0.0477 - 0.0192C_p - 0.0864C_L + 0.0370C_B$ |
| | | 10 | 0.991 | $0.0585 - 0.0232C_p - 0.0929C_L + 0.0353C_B$ |
| | | 30 | 0.985 | $0.0683 - 0.0252C_p - 0.0863C_L + 0.0361C_B$ |
| | | 50 | 0.984 | $0.0689 - 0.0205C_p - 0.0829C_L + 0.0204C_B$ |
| 80 | 0.7 | 5 | 0.993 | $0.0421 - 0.0180C_p - 0.0731C_L + 0.0352C_B$ |
| | | 10 | 0.995 | $0.0528 - 0.0208C_p - 0.0831C_L + 0.0313C_B$ |
| | | 30 | 0.995 | $0.0636 - 0.0225C_p - 0.0798C_L + 0.0232C_B$ |
| | | 50 | 0.992 | $0.0642 - 0.0215C_p - 0.0724C_L + 0.0244C_B$ |
| 100 | 0.8 | 5 | 0.992 | $0.0373 - 0.0202C_p - 0.0523C_L + 0.0348C_B$ |
| | | 10 | 0.997 | $0.0477 - 0.0224C_p - 0.0636C_L + 0.0294C_B$ |
| | | 30 | 0.994 | $0.0586 - 0.0236C_p - 0.0629C_L + 0.0199C_B$ |
| | | 50 | 0.993 | $0.0597 - 0.0219C_p - 0.0589C_L + 0.0188C_B$ |

Table 4 Normalized regression equations relating EHD friction to ^{13}C NMR structural parameters of base oils; (in these regression equations, C_p , C_L and C_B are fractional values, not percentages as in Table 2)

| $T(^{\circ}\text{C})$ | $P(\text{GPa})$ | SRR (%) | Regression equation |
|-----------------------|-----------------|---------|--|
| 40 | 0.6 | 5 | $\mu = 0.0716(1 - 0.360C_p - 1.63C_L + 0.385C_B)$ |
| | | 10 | $\mu = 0.0774(1 - 0.355C_p - 1.45C_L + 0.373C_B)$ |
| | | 30 | $\mu = 0.0800(1 - 0.288C_p - 1.26C_L + 0.391C_B)$ |
| | | 50 | $\mu = 0.0767(1 - 0.280C_p - 1.11C_L + 0.378C_B)$ |
| 60 | 0.6 | 5 | $\mu = 0.0477(1 - 0.403C_p - 1.81C_L + 0.776C_B)$ |
| | | 10 | $\mu = 0.0585(1 - 0.397C_p - 1.59C_L + 0.603C_B)$ |
| | | 30 | $\mu = 0.0683(1 - 0.369C_p - 1.26C_L + 0.529C_B)$ |
| | | 50 | $\mu = 0.0689(1 - 0.300C_p - 1.20C_L + 0.300C_B)$ |
| 80 | 0.7 | 5 | $\mu = 0.0421(1 - 0.428C_p - 1.74C_L + 0.836C_B)$ |
| | | 10 | $\mu = 0.0528(1 - 0.394C_p - 1.57C_L + 0.593C_B)$ |
| | | 30 | $\mu = 0.0636(1 - 0.354C_p - 1.25C_L + 0.365C_B)$ |
| | | 50 | $\mu = 0.0642(1 - 0.335C_p - 1.13C_L + 0.380C_B)$ |
| 100 | 0.8 | 5 | $\mu = 0.0373(1 - 0.542C_p - 1.40C_L + 0.933C_B)$ |
| | | 10 | $\mu = 0.0477(1 - 0.470C_p - 1.33C_L + 0.616C_B)$ |
| | | 30 | $\mu = 0.0586(1 - 0.403C_p - 1.07C_L + 0.340C_B)$ |
| | | 50 | $\mu = 0.0597(1 - 0.367C_p - 0.987C_L + 0.315C_B)$ |

6.9% of naphthenic carbons when a baseline correction is applied as was done for the rest of base oils. However, it was confirmed that the PAO sample has more than 99% paraffinic carbons by the mass spectrometry (MS)-based ASTM test method D2786.

Multiple linear regression analysis between EHD friction and ^{13}C NMR structural parameters of hydrocarbon base oils

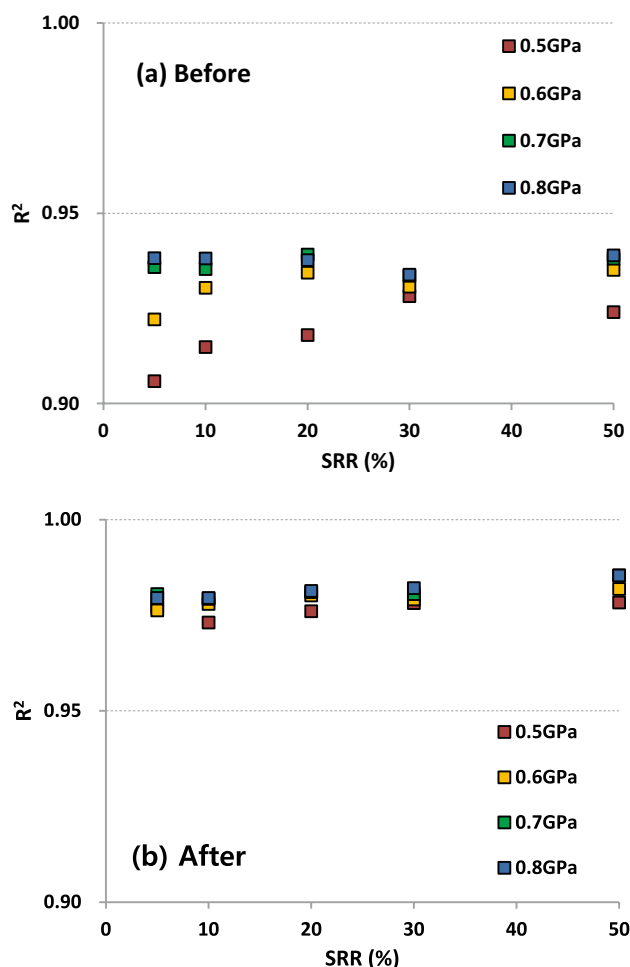


Fig. 11 Regression analysis for EHD friction and ^{13}C NMR structural parameters of base oils at 40 °C, **a** before, **b** after PAO reassignment

including PAO (with C_p : 93.1, C_B : 10.5, C_L : 50.6) give considerably lower R^2 coefficients than when PAO is not included and the average R^2 coefficient falls down to 0.908 (0.925 except for results measured at 0.5 GPa and 0.6 GPa at 120 °C and 0.5 GPa at 100 °C). This can be explained in terms of the unique molecular architecture of PAO, which has long chain branches on a main backbone. Based on the assignment rule applied to ^{13}C NMR, carbons that are located 4 or more carbon atoms away from a backbone chain on long chain branches,

corresponding to ε , δ , γ , β , α in Fig. 4a, are defined as linear carbons, but they are obviously on long branches.

The PAO sample used in this study was polymerized with 1-decene and the ratio of trimer, tetramer and pentamer can be estimated by gas chromatography (trimer 82.2%, tetramer 16.8%, pentamer 1%). Thus, after calculating the number of the linear carbons on long branches and reassigning them as branch carbons (C_p :93.1, C_B :19.9, C_L :41.2), the average R^2 coefficient is improved to 0.966 (0.980 except for results measured at 0.5 GPa and 0.6 GPa at 120 °C and 0.5 GPa at 100 °C), which is close to the R^2 coefficient with mineral oils only. This improvement is shown in Fig. 11 which compares R^2 before and after reassignment.

7 Conclusions

This study shows quantitatively the impact of molecular structures of highly refined hydrocarbon base oils on EHD friction. The relationship between the EHD friction and the molecular structural parameters of base oil has been established with very high R^2 coefficient, especially at high pressure and low and mid-range temperature. The critical average structural parameters for the EHD friction are total paraffin carbons, linear carbons and branched carbons determined by ^{13}C nuclear magnetic resonance (NMR) spectroscopy.

Distinguishable EHD friction curves are achieved depending on API base oils (Group II, II+, III, III+, IV) with similar kinematic viscosity, reflecting the obvious differences in their molecular structures.

Acknowledgements The authors would like thank SK innovation Institute of Technology Innovation for their support for this study.

Open Access This article is licensed under a Creative Commons Attribution 4.0 International License, which permits use, sharing, adaptation, distribution and reproduction in any medium or format, as long as you give appropriate credit to the original author(s) and the source, provide a link to the Creative Commons licence, and indicate if changes were made. The images or other third party material in this article are included in the article's Creative Commons licence, unless indicated otherwise in a credit line to the material. If material is not included in the article's Creative Commons licence and your intended use is not permitted by statutory regulation or exceeds the permitted use, you will need to obtain permission directly from the copyright holder. To view a copy of this licence, visit <http://creativecommons.org/licenses/by/4.0/>.

Appendix

See Figs. 12 and 13.

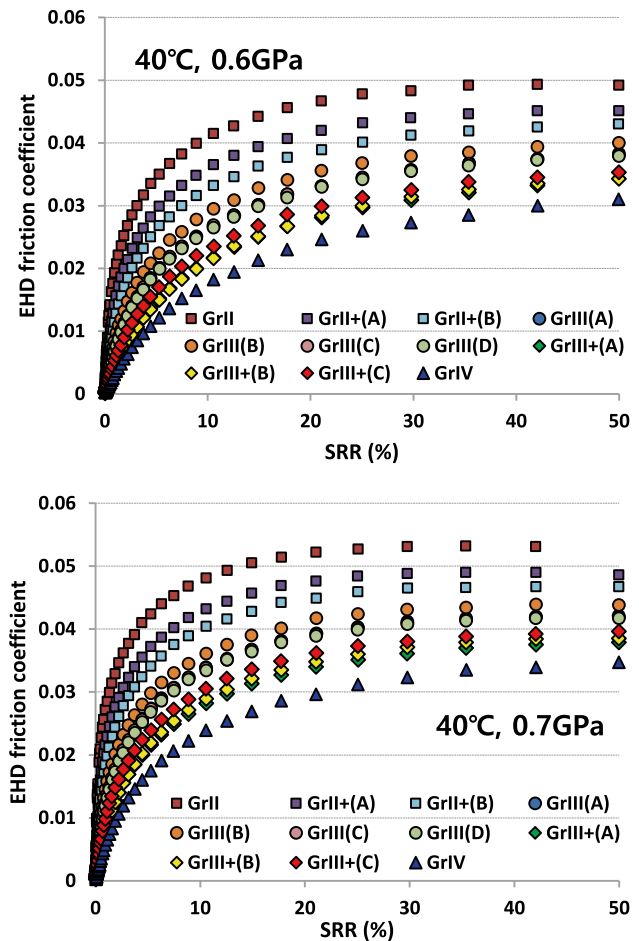


Fig. 12 EHD friction data for hydrocarbon base oils at all conditions tested

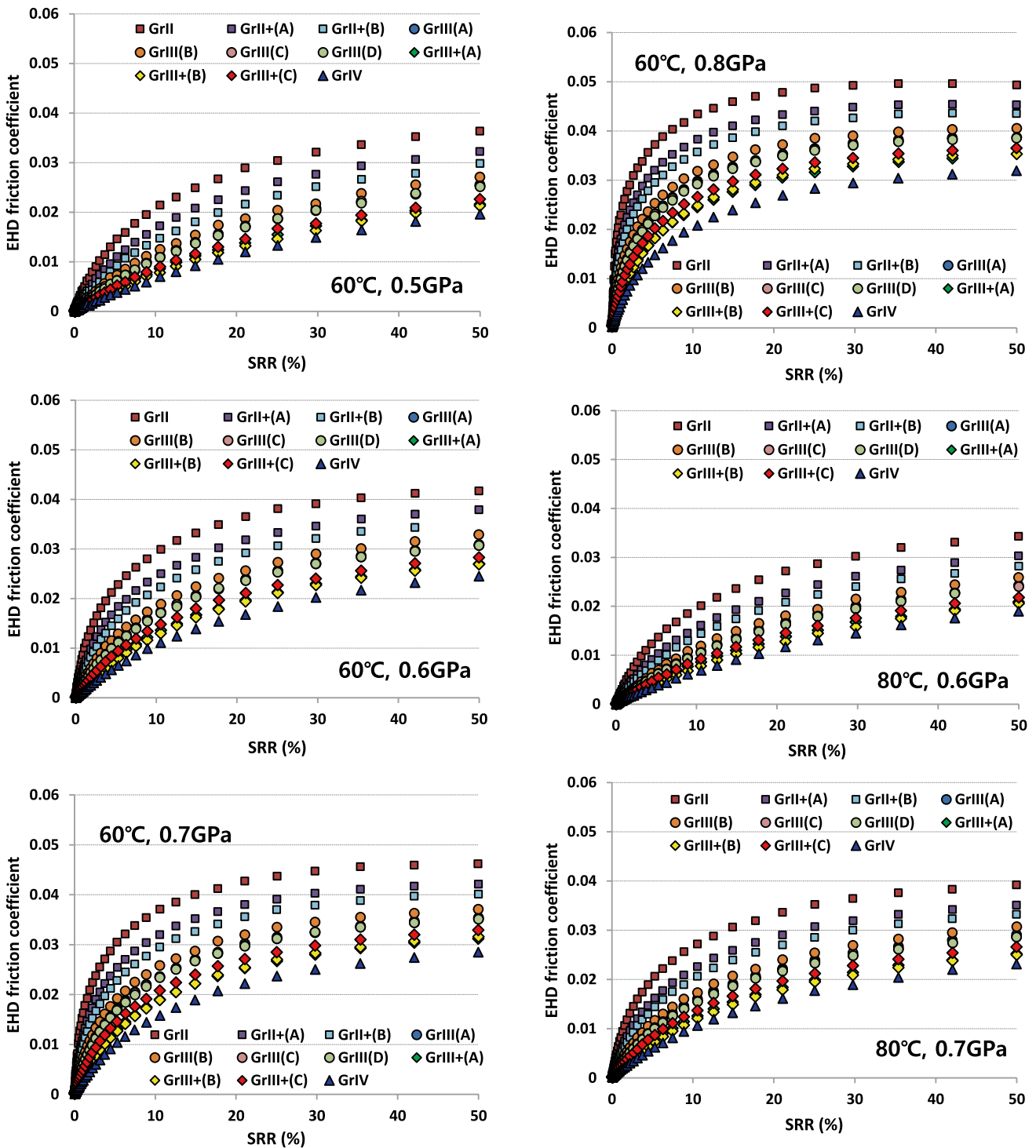


Fig. 12 (continued)

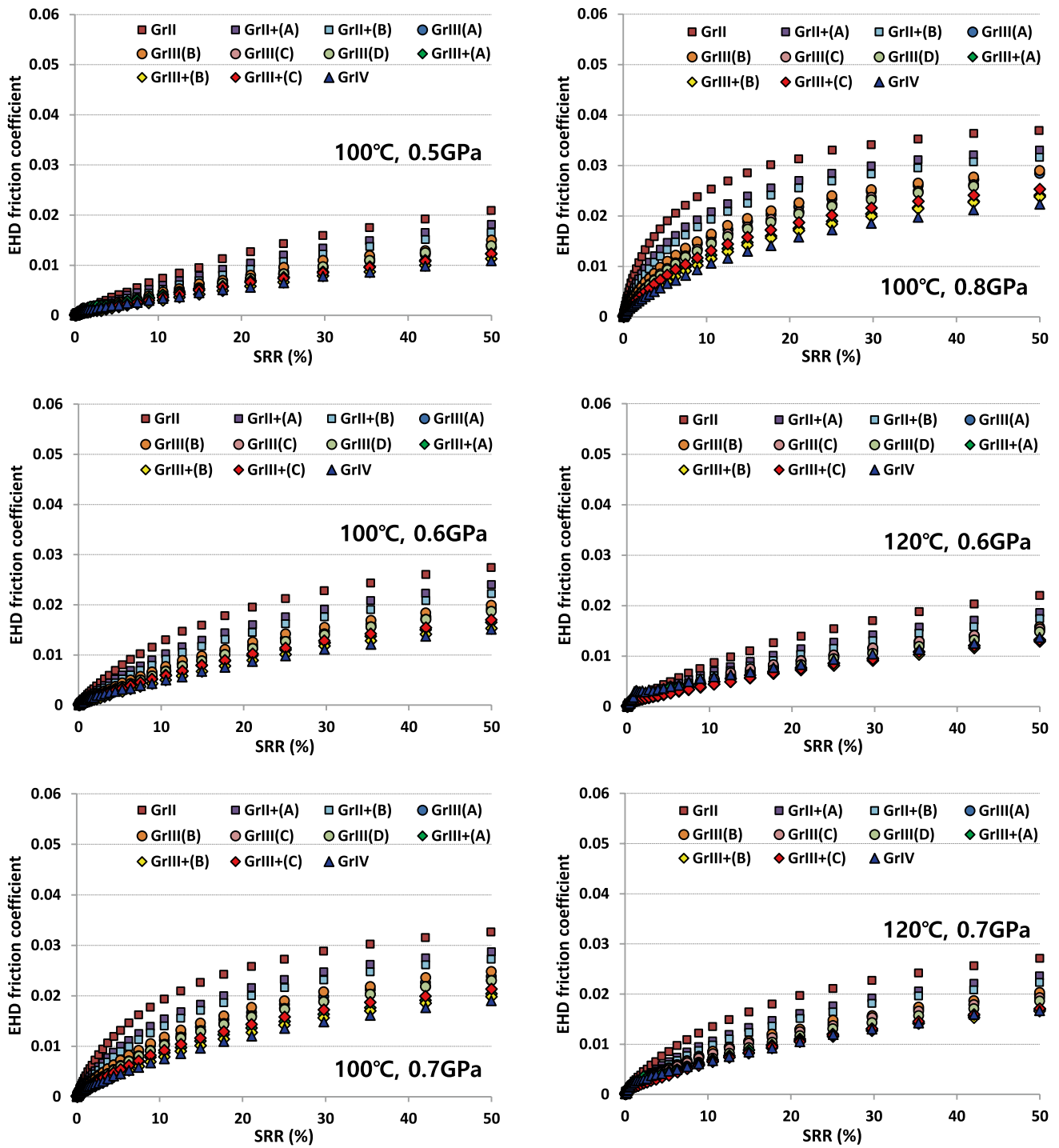


Fig. 12 (continued)

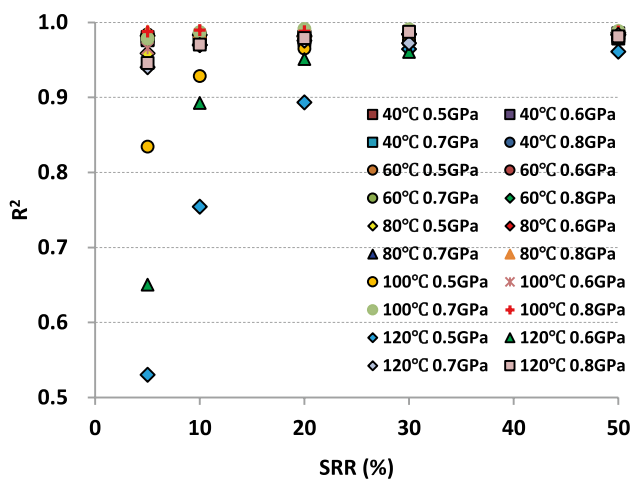


Fig. 13 Regression analysis data for EHD friction and ^{13}C NMR structural parameters of hydrocarbon base oils

References

- Hsu, C.S., Robinson, P.R.: Petroleum science and technology. Springer, Cham (2019)
- Zhang, J., Tan, A., Spikes, H.A.: Effect of base oil structure on elastohydrodynamic friction. *Tribol. Lett.* **65**, 13 (2017)
- Hammann, W.C., Schisla, R.M., Groenweghe, L.C.D., Gash, V.W.: Synthetic fluids for high capacity traction drives. *ASLE Trans.* **13**, 105–116 (1970)
- Muraki, M.: Molecular structure of synthetic hydrocarbon oils and their rheological properties governing traction characteristics. *Tribol. Int.* **20**, 347–354 (1987)
- Smeeth, M., Gunsels, S., Korcek, S.G., Spikes, H.A.: The elastohydrodynamic friction and film-forming properties of lubricant base oils. *Tribol. Trans.* **42**, 559–569 (1999)
- Hentschel, K.-H.: The influence of molecular structure on the frictional behaviour of lubricating fluids. *J. Synth. Lubr.* **2**, 143–174 (1985)
- Tsubouchi, T., Hata, H.: The fundamental molecular structures of synthetic traction fluids. *Tribol. Int.* **27**, 183–187 (1994)
- Tsubouchi, T., Hata, H.: Study on the fundamental molecular structures of synthetic traction fluids: part 2. *Tribol. Int.* **28**, 335–340 (1995)
- Hata, H., Tsubouchi, T.: Molecular structures of traction fluids in relation to traction properties. *Tribol. Lett.* **5**, 69–74 (1998)
- Tsubouchi, T., Hata, H., Yoshida, Y.: Optimisation of molecular structure for traction fluids. *Lubr. Sci.* **16**, 393–403 (2004)
- Edgar, J.A., Hurley, S.: The use of quantitative structure activity relationships (QSAR) in traction fluid design. *SAE Tech. Pap.* **37**, 1484–1491 (2004)
- Hentschel, K.-H.: The influence of molecular structure on the frictional behaviour of lubricating fluids 2: low coefficients of traction. *J. Synth. Lubr.* **2**, 238–260 (1985)
- Chang, H.-S., Bunemann, T., Spikes, H.A.: The shear stress properties of ester lubricants in elastohydrodynamic contacts. *J. Synth. Lubr.* **9**, 91–114 (1992)
- Rounds, F.G.: Effects of lubricant composition on friction as measured with thrust ball bearings. *J. Chem. Eng. Data* **5**, 499–507 (1960)
- Yang, S., Reddyhoff, T., Spikes, H.A.: Influence of lubricant properties on ARKL temperature rise and transmission efficiency. *Tribol. Trans.* **56**, 1119–1136 (2013)
- Yoshizaki, M., Naruse, C., Nemoto, R., Haizuka, S.: Study on frictional loss of spur gears (concerning the influence of tooth form, load, tooth surface roughness, and lubricating oil). *Tribol. Trans.* **34**, 138–146 (1991)
- Michaelis, K., Höhn, B.R., Hinterstoißer, M.: Influence factors on gearbox power loss. *Ind. Lubr. Tribol.* **63**, 46–55 (2011)
- Sarpal, A.S., Kapur, G.S., Chopra, A., Jain, S.K., Srivastava, S.P.: Hydrocarbon characterization of hydrocracked base stocks by one- and two-dimensional NMR spectroscopy. *Fuel* **75**, 483–490 (1996)
- Sharma, B.K., Stipanovic, A.J.: Pressure viscosity coefficient of lubricant base oils as estimated by nuclear magnetic resonance spectroscopy. *Ind. Eng. Chem. Res.* **41**, 4889 (2002)
- Sharma, B.K., Stipanovic, A.J.: Predicting low temperature lubricant rheology using nuclear magnetic resonance spectroscopy and mass spectrometry. *Tribol Lett* **16**, 11–19 (2004)
- Papke, B.L., Tutunjian, P.N.: Application of ^{13}C -NMR to predict low temperature viscosity performance of base oils. *Tribotest.* **12**, 211–222 (2006)
- Sharma, B.K., Adhvaryu, A., Perez, J.M., Erhan, S.Z.: Effects of hydroprocessing on structure and properties of base oils using NMR. *Fuel Process Technol* **89**, 984–991 (2008)
- API base oil interchangeability guidelines for passenger car motor oils and diesel engine oils, Annex E, American Petroleum Institute (API) Publication 1509 (2019)
- Johnston, G.J., Wayte, R., Spikes, H.A.: The measurement and study of very thin lubricant films in concentrated contacts. *Trib. Trans.* **34**, 187–194 (1991)
- Hamrock, B.J., Dowson, D.: Ball Bearing Lubrication. The Elastohydrodynamics of Elliptical Contacts. Wiley, New York (1981)
- Johnson, K.L., Tevaarwerk, J.L.: Shear behaviour of elastohydrodynamic films. *Proc. R. Soc. Lond.* **A356**, 215–238 (1977)
- Spikes, H.A., Zhang, J.: History, origins and prediction of elastohydrodynamic friction. *Tribol. Lett.* **56**, 1–25 (2014)
- Larsson, R., Andersson, O.: Lubricant thermal conductivity and heat capacity under high pressure. *Proc. Inst. Mech. Eng. J* **214**, 337–342 (2000)
- Evans, C.R., Johnson, K.L.: The rheological properties of elastohydrodynamic lubricants. *Proc. Inst. Mech. Eng.* **C200**, 303–312 (1986)
- Evans, C.R., Johnson, K.L.: Regimes of traction in elastohydrodynamic lubrication. *Proc. Inst. Mech. Eng.* **C200**, 313–324 (1986)

Publisher's Note Springer Nature remains neutral with regard to jurisdictional claims in published maps and institutional affiliations.